DESIGN AND FABRICATION OF AN INTEGRATED PROGRAMMABLE FLOATING-GATE MICROPHONE

Tengge Ma, Tsz Yin Man, Yick Chuen Chan*, Yitshak Zohar* and Man Wong

Department of Electrical & Electronic Engineering, *Department of Mechanical Engineering
The Hong Kong University of Science and Technology, Clear Water Bay, Kowloon, Hong Kong

ABSTRACT

An integrated, programmable floating-gate capacitive microphone has been designed and fabricated. The conducting floating-gate is electrically insulated and is "programmed" by injecting electrons into it using Fowler-Nordheim tunneling through a thin silicon dioxide film, thus capable of simulating an electret and generating a permanent electric field. A current-driving buffer based on metal-oxide-semiconductor field-effect transistors is integrated to reduce the capacitive loading of the microphone. The fabrication process is MOS compatible and promises the potential of integrating a variety of signal processing electronic circuits.

INTRODUCTION

Miniaturized microphones can be found in a range of applications such as cell phones, hearing aids, smart toys and surveillance devices, etc. Allowing batch fabrication and integration of miniaturized devices with different functions, micro-fabrication is uniquely suitable for realizing inexpensive micro-systems with enhanced capabilities. Several types of silicon microphones, such as piezo-electric, piezo-resistive and capacitive (including electret) microphones [1] have been investigated.

Higher sensitivity is the principal advantage of capacitive over piezo-electric and piezo-resistive sensing. Furthermore, if permanent storage of charges were possible, as in an electret capacitor, external biasing network could be eliminated. Unfortunately, most electrets are incompatible with the micro-fabrication of metal-oxide-semiconductor (MOS) devices, making it difficult to integrate electronic devices with electret microphones. A further disadvantage is that most electret capacitors are not electrically programmable, making it impossible to electrically regenerate any charges lost after their initial storage on the capacitor.

The design, fabrication and characterization of an integrated, programmable floating-gate capacitive microphone are presented. Its micro-fabrication is a one-wafer process requiring no wafer bonding. Instead of an electret [2], an electrically insulated conducting floating-gate is used as one of the capacitor plates in the microphone to generate the desired permanent electric field and as the gate of the read-out transistor. The electrons on the floating-gate are electrically injected and replenished using Fowler-Nordheim (FN) tunneling mechanism. A simple buffer circuit is integrated to reduce the parasitic capacitance. Obviously, more sophisticated signal-processing circuits can be incorporated, since the process is intrinsically MOS compatible.

MODELLING AND SIMULATIONS

The voltage necessary for FN tunneling of electrons into the floating-gate (V_f) is induced by a bias (V_c) applied to the counter-electrode (control-gate) of the sensing capacitor. The efficiency of the voltage transfer is parameterized by the coupling ratio (V_f/V_c). The electrical equivalent circuit of the floating-gate microphone is shown in Figure 1.

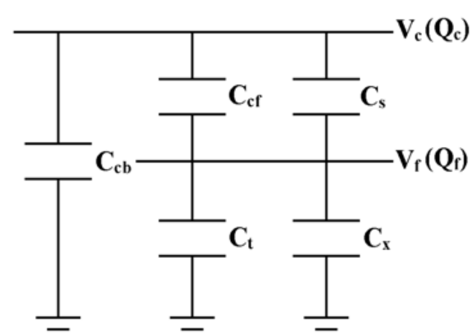

Figure 1. An electrical equivalent circuit of the integrated floating-gate microphone.

C_s, C_t and C_x represent respectively the capacitance associated with the sensing capacitor, the tunnel oxide and the input transistor of the current buffer. C_{cb} and C_{cf} are, respectively, the substrate to control-gate and the substrate to floating-gate capacitance. Initially, the floating-gate is not charged,

(1) $$Q_c = V_c\left[C_{cb} + \left(C_t + C_x\right)//\left(C_{cf} + C_s\right)\right],$$

(2) $$Q_c = V_c C_{cb} + Q_f,$$

(3) $$Q_f = V_f\left(C_t + C_x\right),$$

where Q_c and Q_f are charges on the control-gate and the floating-gate, respectively. From (2) and (3),

$$Q_c = V_c C_{cb} + V_f \left(C_t + C_x\right). \tag{4}$$

Equating (1) and (4), one obtains for the coupling ratio

$$\frac{V_f}{V_c} = \frac{C_{cf} + C_s}{C_{cf} + C_s + C_t + C_x}. \tag{5}$$

In the present implementation, C_s is the dominant capacitance and the coupling ratio can be made large and close to 1.

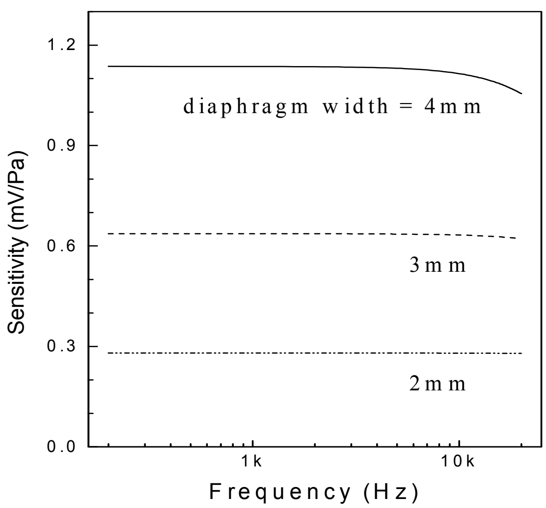

Figure 2. Simulated dependence of the frequency response of the integrated floating-gate microphone on membrane size.

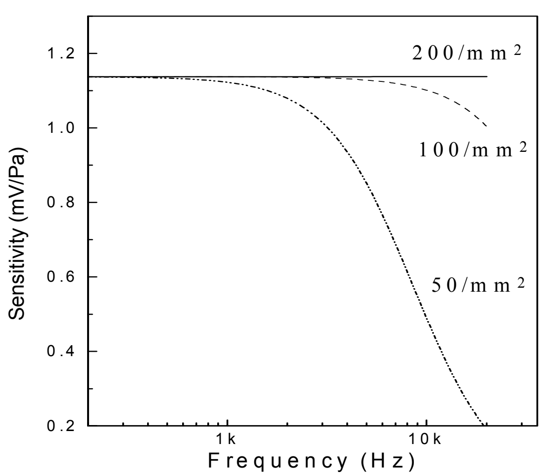

Figure 3. Simulated dependence of the frequency response of the integrated floating-gate microphone on ventilation hole density.

The response of the floating-gate microphone has been simulated using an electrical equivalent circuit, taking into account the contribution of the acoustic pressure loading (P), the diaphragm, the air-gap, the ventilation holes and the back-plate. The sensitivity of the microphone is the output voltage (V_o) of the sensing capacitor, before amplification, divided by P. Six parameters have been considered in the design: diaphragm area and thickness, air gap and back-plate thickness, ventilation hole size and density. The performance of the device improves with increasing diaphragm size (Fig. 2) and increasing ventilation hole density (Fig. 3).

MICROPHONE FABRICATION

The major steps of the fabrication process for the microphone are illustrated in Figure 4.

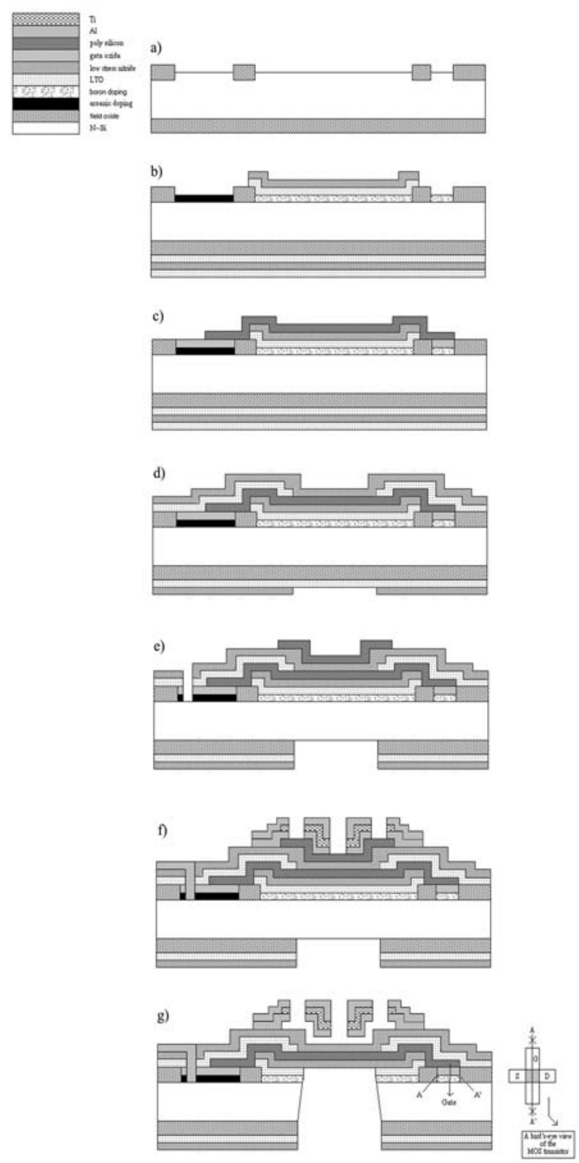

Figure 4. Process flow for the integrated programmable floating-gate microphone.

The starting substrates were double-side polished n-type (100) silicon wafers. Thermal oxidation was used to form thick field-oxide for device isolation (Fig. 4a). Subsequently, boron was implanted to adjust the threshold voltage of the MOS field-effect transistors (FETs) and arsenic was implanted to form the highly doped regions for substrate contact and FN tunneling window.

A first layer of low-stress nitride (Si_xN_y) was deposited and patterned (Fig. 4b). This was followed by the formation of gate and tunnel oxides. Subsequently, poly-Si was deposited and patterned to form the gate electrodes for the FETs and the floating-gate for the sensing capacitors (Fig. 4c). A second layer of Si_xN_y, similar in thickness to that of the first nitride, was deposited to insulate the floating-gate and to form a stress-balanced Si_xN_y/poly-Si/Si_xN_y sandwich sensing membrane.

Before the deposition and patterning of the poly-Si sacrificial layer, the backside of the wafer was patterned to prepare the device for the deep silicon through-hole etch (Fig. 4d). This choice of sacrificial material allows simultaneous formation of the air-gap and the realization of the membrane of the sensing capacitor during the final through-hole etch.

The contact holes were opened (Fig. 4e) before the formation of the stress-balanced and structurally reinforced Al/Ti/Al metal multi-layer. These metal layers serve both as the counter-electrode for the sensing capacitor and the interconnection for the electronic devices (Fig. 4f). Ventilation holes were patterned in the counter-electrode to reduce air damping.

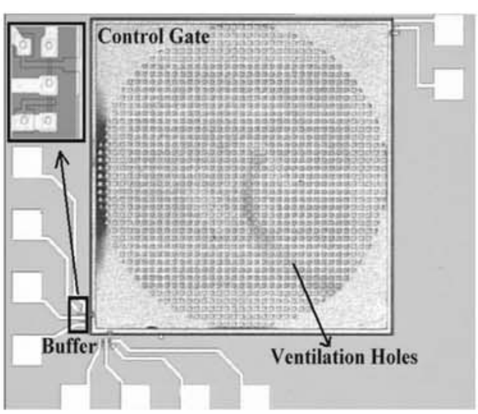

Figure 5. Photograph of a completed integrated floating-gate microphone. A magnified view of the buffer is shown in the inset.

Finally, the poly-Si sacrificial layer between the electrodes and the bulk silicon to which the bottom nitride of the sensing membrane was attached were etched in a modified tetra-methyl ammonium hydroxide (TMAH) solution with very high silicon to aluminum etch selectivity [3]. This final membrane release (Fig. 4g) was performed after the completion of all front side processing of the wafer, including metal formation. Consequently, it is more compatible with conventional MOS foundry processes than a previously reported floating-gate device [4].

The photograph of a fabricated device, showing the current-driving buffer and the counter-electrode (control-gate) perforated with ventilation holes, is presented in Figure 5.

CHARACTERIZATIONS

The output, i.e. drain current (I_d) *vs* drain voltage (V_d), characteristics of a transistor and the voltage transfer, i.e. output voltage (V_o) *vs* input voltage (V_i), characteristic of a current-driving buffer are shown in Figures 6 and 7, respectively.

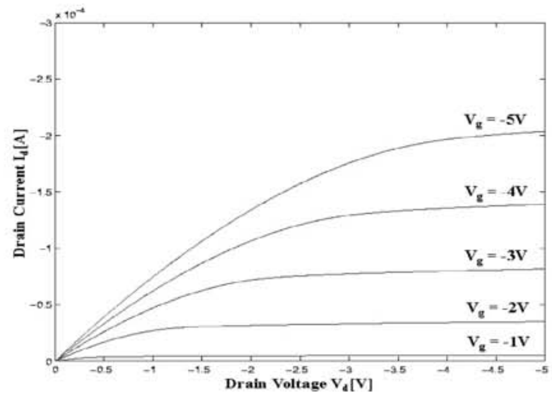

Figure 6. Output (I_d-V_d) characteristic of a MOSFET.

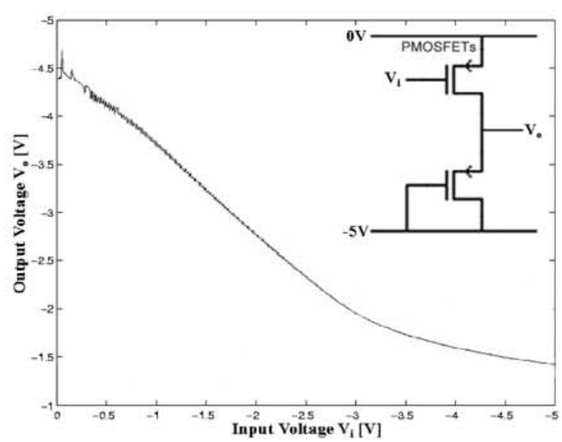

Figure 7. Voltage transfer (V_o-V_i) characteristic of a current-driving buffer.

These characteristics are well-behaved, demonstrating that the electronic devices can be integrated with the microphone using the proposed micro-fabrication processes.

The tunnel oxide was characterized using a ramped voltage test to determine the threshold voltage (V_{st}) for tunneling and the breakdown voltage (V_{BD}) at which the oxide would be irrecoverably destroyed. From Figure 8, V_{st} is around 18V and V_{BD} is larger than 30V. Consequently, 25V was selected to obtain a fast charge injection time, while reducing the chance of pre-mature oxide breakdown.

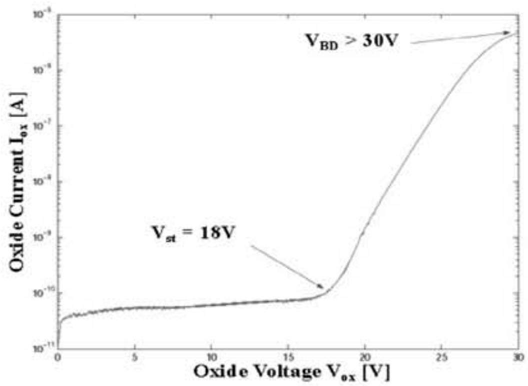

Figure 8. I-V characteristic of tunneling oxide.

The coupling ratio of the control and floating gates was determined to be 0.67, showing that for the particular device measured, the parasitic capacitance was still significant. Combining the coupling ratio and the desired initial floating-gate voltage, the voltage applied to the control-gate was chosen to be 37V.

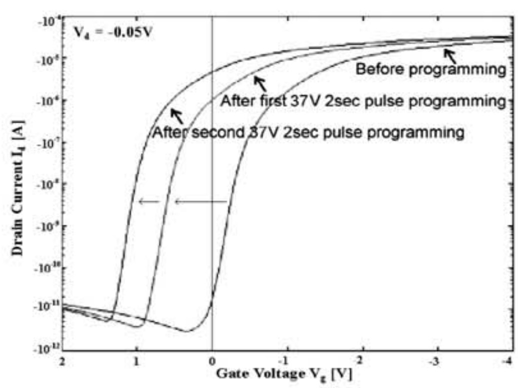

Figure 9. Shifts of I_d-V_g characteristics as a function of injected charge.

The shifts in the transfer characteristics, i.e. I_d *vs* gate voltage (V_g), in response to the number of 37V, 2sec "programming" pulses applied to the control-gate are shown in Figure 9. As expected, a stored-electron induced positive shift in transistor threshold voltage was obtained after the application of the programming pulse. More electrons, hence more positive shift was obtained after a second pulse. This charge is permanently stored on the electrically insulated floating-gate.

The measured response of the programmable floating-gate microphone is shown in Figure 10. When the sensing membrane is excited by acoustic signals, the change in the capacitance of the sensing capacitor is converted to a voltage signal, since the floating-gate provides a relatively constant electric field due to the injected charge. Finally, the change in the voltage is converted by the current-buffer to a measurable current signal.

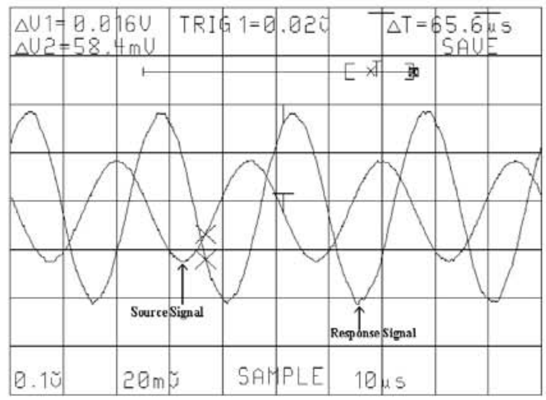

Figure 10. Measured response of the integrated floating-gate microphone.

CONCLUSION

A programmable floating-gate microphone with integrated electronic signal processing electronic devices has been designed, simulated and implemented using an MOS-compatible fabrication process.

REFERENCES

[1] P.R. Scheeper, A.G.H. van der Donk, W. Olthuis, P. Bergveld, *Sensors and Actuators A,* 44 (1994) 1-11.

[2] W.H. Hsieh, T.Y. Hsu, Y.C.Tai, 1999 *Proc.10th Int. Conf. On Solid-State Sensors & Actuators*, pp.1064-1067.

[3] G.Z. Yan, P.C.H. Chan, I.M. Hsing, R.K. Sarma, J.K.O. Sin, 2000 *13th Int. Micro Electro Mechanical Systems Conf.*, pp. 562-567.

[4] Q.B. Zou, Z.M. Tan, Z.F. Wang, M.K. Lim, R.M. Lin, S.Yi, Z.J. Li, 1998 *Proc. 11th Int. Micro Electro Mechanical Systems Conf.*, pp. 586-590.